

Yong HAN, Feng LIU

## Coulomb sink effect on coarsening of metal nanostructures on surfaces

© Higher Education Press and Springer-Verlag 2008

**Abstract** We discuss Coulomb effects on the coarsening of metal nanostructures on surfaces. We have proposed a new concept of a “Coulomb sink” [Phys. Rev. Lett., 2004, 93: 106102] to elucidate the effect of Coulomb charging on the coarsening of metal mesas grown on semiconductor surfaces. A charged mesa, due to its reduced chemical potential, acts as a Coulomb sink and grows at the expense of neighboring neutral mesas. The Coulomb sink provides a potentially useful method for the controlled fabrication of metal nanostructures. In this article, we will describe in detail the proposed physical models, which can explain qualitatively the most salient features of coarsening of charged Pb mesas on the Si(111) surface, as observed by scanning tunneling microscopy (STM). We will also describe a method of precisely fabricating large-scale nanocrystals with well-defined shape and size. By using the Coulomb sink effect, the artificial center-full-hollowed or half-hollowed nanowells can be created.

**Keywords** Coulomb sink, metal nanostructures, coarsening, STM

**PACS numbers** 81.07.Bc, 81.10.Aj, 68.43.Jk

### 1 Introduction

The development of nanoelectronic devices requires con-

trolled fabrication of nanostructures on the surface. Two parallel routes have been taken toward this goal: one is the top-down approach, such as nanopatterning, and the other is the bottom-up approach, such as self-assembly. In this article, we will demonstrate a novel effect of Coulomb charging on the coarsening of metal nanoclusters on surfaces, providing a potentially useful method for controlled fabrication of metal nanostructures.

The Coulomb effect is ubiquitous in physics, chemistry, and biology. One well-known manifestation of the Coulomb effect on the stability of a cluster is Coulomb explosion. It is defined classically by the Rayleigh instability limit [1], above which an excessively charged cluster becomes unstable and explodes into smaller fragments. For a nanocluster, the critical size for Coulomb explosion depends on the nature of chemical bonding [2].

When a metal cluster is charged on a surface, it may not explode, but instead grow its size by “sinking” atoms from its neighboring neutral clusters to reduce its Coulomb energy. We call this effect the “Coulomb sink”. The first experimental evidence of the Coulomb sink is from Okamoto *et al.* [3], who attributed this phenomenon to the high Maxwell stress of the local electrical field lines which draw the atom towards the high field region on top of the island. However, their theoretical explanation was unsuccessful [3]. In the following sections, we will elaborate, by both theory and experiment, on the phenomena of Coulomb sink with metal nanomesas grown on insulator and semiconductor surfaces. The basic viewpoint is that charging can reduce the chemical potential of the charged mesa relative to its neighboring neutral mesas, and consequently it grows at the expense of its neighbors via a coarsening process. Because one can selectively charge any chosen mesa with a controllable amount of charge, *Coulomb sink provides a unique and effective method for manipulating the growth of metal mesas with a size control up to millions of atoms.*

Yong HAN<sup>1,2</sup>, Feng LIU<sup>2</sup> (✉)

<sup>1</sup> IPR and Ames Laboratory, U. S. Department of Energy, 307D Wilhelm Hall, Ames, IA 50011, USA

<sup>2</sup> Department of Materials Science and Engineering, University of Utah, Salt Lake City, UT 84112, USA  
E-mail: octavian2009@gmail.com; fliu@eng.utah.edu

Received November 14, 2007; accepted December 8, 2007

## 2 Theoretical models

### 2.1 Hemisphere-capacitor model

The capacitance of a conductor monotonously increases as a function of its size. Thus, to lower its Coulomb energy, the charged mesa (cluster in general) may increase its size to maximize its capacitance. For coarsening, this implies that the chemical potential of the charged cluster is instantaneously reduced, with respect to its neighboring uncharged clusters, so it grows at the expense of its neighbors. Let us consider a metal cluster in a hemisphere shape with radius  $R$  grown on an insulator surface, as shown in Fig. 1. If the cluster is neutral, the energy in reference to the bare surface is

$$E_0 = \pi R^2(\gamma_{\text{int}} - \gamma_{\text{sub}} + 2\gamma_{\text{sph}}) \equiv \pi R^2\alpha \quad (1)$$

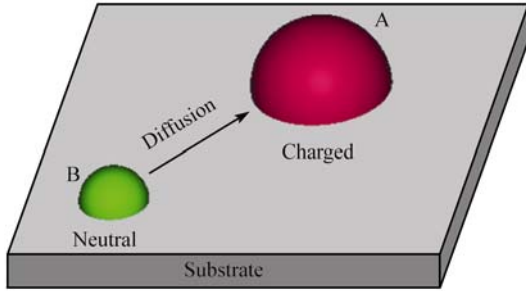


**Fig. 1** (Color online) Schematic illustration of the Coulomb sink. On the insulator substrate, the atoms of neutral cluster B diffuse onto charged cluster A in a coarsening process.

where  $\gamma_{\text{int}}$ ,  $\gamma_{\text{sub}}$  and  $\gamma_{\text{sph}}$  are the cluster-substrate interface energy, the substrate surface energy, and the cluster surface energy, respectively. The chemical potential can be defined as

$$\mu_0 = \frac{dE_0}{dN} = \Omega \frac{dE_0}{dV} = \Omega \frac{\alpha}{R} \quad (2)$$

where  $\Omega$  is the atomic volume,  $V$  is the volume of the hemisphere cluster,  $N$  is the total number of atoms in the hemisphere. In writing Eq. (2), the relation

$$V = N\Omega = \frac{2}{3}\pi R^3 \quad (3)$$

and Eq. (1) have been used.

When an isolated conductor is charged with  $Q$ , the excessive Coulomb energy is

$$E_c = \frac{Q^2}{2C} \quad (4)$$

where  $C$  is the capacitance of the isolated conductor. Now, for a hemisphere conductor charged with  $Q$ , its Coulomb energy is

$$E_c = \frac{Q^2}{4\pi\epsilon R} \quad (5)$$

where  $\epsilon$  is the dielectric constant. Therefore, the total energy of the charged cluster is

$$E = E_0 + E_c = \pi R^2\alpha + \frac{Q^2}{4\pi\epsilon R} \quad (6)$$

Here, the capacitance of the metal hemisphere has been assumed to be  $C = 2\pi\epsilon R$ . Then, the chemical potential becomes

$$\mu = \frac{dE}{dN} = \Omega \frac{dE}{dV} = \Omega \left( \frac{\alpha}{R} - \frac{Q^2}{8\pi^2\epsilon R^4} \right) \quad (7)$$

Now, consider two metal nano-hemisphere clusters, A and B, with the same initial radius  $R$ . Let A be charged by  $Q$ , and B is neutral. Apparently, the chemical potential of A will be reduced by  $\frac{\Omega Q^2}{8\pi^2\epsilon R^4}$ , as expressed in Eq. (7). It follows that the atoms of B will diffuse onto A in a coarsening process, i.e., the charged cluster A *sinks* the atoms from the neutral cluster B. During the process of coarsening, the system total energy is

$$E_{\text{tot}} = \pi R_A^2\alpha + \frac{Q^2}{4\pi\epsilon R_A} + \pi R_B^2\alpha \quad (8)$$

where  $R_A$  and  $R_B$  are the radii of A and B, respectively. Also, the volume conservation requires

$$V_{\text{tot}} = \frac{4}{3}\pi R^3 = \frac{2}{3}\pi(R_A^3 + R_B^3) \quad (9)$$

From Eqs. (8) and (9), it is shown that the minimum of  $E_{\text{tot}}$  is at  $R_B = 0$ , and then the maximum of  $R_A$  equals to  $2^{1/3}R \approx 1.26R$ . This indicates that the neutral cluster will eventually disappear.

### 2.2 Cylinder-capacitor model

The growth of metal film on semiconductor substrates proceeds via Volmer-Weber mode [4, 5], forming three-dimensional (3D) islands, when the surface energy of the film is much higher than that of the substrate. The islands may adopt an equilibrium mesa shape defined by surface energy anisotropy, such as Au mesas on C(0001) surface [6] and Pb mesas on Si(111) surface [7–9]. For simplicity, however, we assume a mesa has the perfect cylindrical shape with radius  $R$  and height  $H$ , as shown in Fig. 2. The energy of a neutral mesa, in reference to a bare surface, is then

$$E_0 = \pi R^2\alpha_1 + 2\pi RH\alpha_2 \quad (10)$$

where  $\alpha_1 = \gamma_{\text{mt}} + \gamma_{\text{int}} - \gamma_{\text{sub}}$  and  $\alpha_2 = \gamma_{\text{ms}}$ . Here,  $\gamma_{\text{mt}}$  and  $\gamma_{\text{ms}}$  are, respectively, the surface energy of the mesa top and the

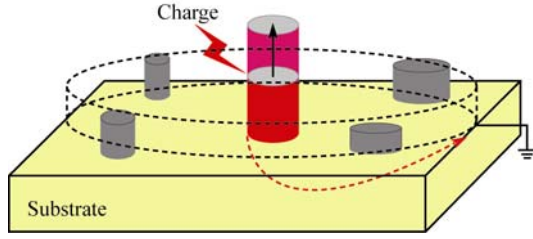


**Fig. 2** (Color online) Schematic illustration of a cylindrical capacitor formed by a charged metal mesa and the distant groundings (dotted lines). The dashed arrow line indicates the discharging process: the arrowed part of the cylinder indicates the height growth of the charged mesa.

mesa sidewall, and  $\gamma_{\text{int}}$  and  $\gamma_{\text{sub}}$  are, respectively, mesa-substrate interface energy and substrate surface energy.

Now, consider one chosen mesa is charged by  $Q$ , using a scanning tunneling microscope (STM), and the charge will subsequently discharge to the substrate within a period of time, as illustrated in Fig. 2. By considering a capacitor formed between the charged mesa and its surroundings, its energy is instantaneously increased by  $E_c$  [Eq. (4)].

Based on the mesa geometry, we model the charging effect by a coaxial cylindrical capacitor of height  $H$ , as shown in Fig. 2. The inner conductor is the charged mesa having a radius  $R$  with charge  $Q$ , and the outer conducting shell (dotted lines) represents the distant groundings, having a much larger radius  $R_g$ . Its capacitance is then calculated as

$$C = \frac{2\pi\epsilon}{\ln(R_g/R)} H \quad (11)$$

where  $\epsilon$  is the dielectric constant. Therefore, the excessive Coulomb energy of the charged mesa is

$$E_c = \frac{\ln(R_g/R)}{4\pi\epsilon} \frac{Q^2}{H} \quad (12)$$

Thus, from Eqs. (10) and (12), the total energy of a charged mesa is

$$E = E_0 + E_c = \pi R^2 \alpha_1 + 2\pi R H \alpha_2 + \frac{\ln(R_g/R)}{4\pi\epsilon} \frac{Q^2}{H} \quad (13)$$

An increase of either  $H$  or  $R$  results in a decrease of  $E$ . To specify the growth of height versus radius, we define a ‘‘partial’’ chemical potential for height growth as

$$\mu_H = \left( \frac{\partial E}{\partial N} \right)_R = \Omega \left( \frac{\partial E}{\partial V} \right)_R = \Omega \frac{2\alpha_2}{R} - \Omega \frac{\ln(R_g/R)}{4\pi^2\epsilon R^2} \frac{Q^2}{H^2} \quad (14)$$

representing the change of Coulomb energy with respect to changing height at a fixed radius, and a ‘‘partial’’ chemical potential for radius growth as

$$\mu_R = \left( \frac{\partial E}{\partial N} \right)_H = \Omega \left( \frac{\partial E}{\partial V} \right)_H = \Omega \left( \frac{\alpha_1}{H} + \frac{\alpha_2}{R} \right) - \frac{\Omega}{8\pi^2\epsilon R^2} \frac{Q^2}{H^2} \quad (15)$$

representing the change of Coulomb energy with respect to changing radius at fixed height. Here,  $\Omega$  is the atomic volume,  $V$  is the volume of the charged mesa, and  $N$  is the total number of atoms contained in the mesa. Also, in writing Eqs. (14) and (15), we have used Eq. (13) and the relation  $V = N\Omega = \pi R^2 H$ . From Eqs. (14) and (15), a growth index function can be defined as

$$S = \mu_H - \mu_R = \Omega \left( \frac{\alpha_2}{R} - \frac{\alpha_1}{H} \right) - \frac{\Omega}{8\pi^2\epsilon R^2} \frac{Q^2}{H^2} \left( 2 \ln \frac{R_g}{R} - 1 \right) \quad (16)$$

which tells the energetically favored growth direction. It can be easily verified that if  $Q$  is not too small, the surface tension effects can be neglected, and then Eqs. (14), (15), and (16) become

$$\mu_H = -\Omega \frac{\ln(R_g/R)}{4\pi^2\epsilon R^2} \frac{Q^2}{H^2} \quad (17)$$

$$\mu_R = \frac{\Omega}{8\pi^2\epsilon R^2} \frac{Q^2}{H^2} \quad (18)$$

and

$$S = \mu_H - \mu_R = -\frac{\Omega}{8\pi^2\epsilon R^2} \frac{Q^2}{H^2} \left( 2 \ln \frac{R_g}{R} - 1 \right) \quad (19)$$

respectively. Because  $R_g \gg R$ ,  $S < 0$ . It is readily seen from Eq. (19) that the charged mesa always favors growth in height.

Charging affects coarsening by breaking down the chemical-potential balance between the original neutral mesas, because the energy of the charged mesa is decreased by an amount  $\sim Q^2$ . It makes the charged mesa act effectively as a Coulomb sink to attract atoms from the surrounding neutral mesas. Therefore, it triggers the otherwise ‘‘ceased’’ coarsening process by creating a high supersaturation around the charge mesa to overcome the energy barrier for nucleating new layers [7, 8, 10] to grow in height. To assess the amount of growth induced by charging, we consider the coarsening process to be controlled by the attachment of adatoms to the mesa [11], and assume that the rate of volume growth is simply proportional to the chemical-potential difference between the charged mesa and the surrounding neutral mesas. It follows that the rate of height growth can be expressed as

$$\frac{dH}{dt} = -\frac{\sigma}{\pi R^2} (\mu - \bar{\mu}) \quad (20)$$

where  $\sigma$  is a coefficient related to the adatom attachment rate and the atomic volume,  $\mu$  is the chemical potential of the charged mesa, and  $\bar{\mu}$  is the mean chemical potential of

the surrounding neutral mesas. The proportionality coefficient  $\sigma$  can be estimated by

$$\sigma = \frac{\Omega}{kT} \nu e^{-\Delta/kT} \quad (21)$$

where  $\Delta$  is the energy barrier of attachment,  $k$  is Boltzmann's constant, and  $\nu$  is the atom-jumping attempt frequency. If  $\nu$  is approximately taken as  $kT/h$ , where  $h$  is Planck's constant, and  $T$  is temperature, then Eq. (21) can be rewritten as

$$\sigma = \frac{\Omega}{h} e^{-\Delta/kT} \quad (22)$$

From the fundamental thermodynamic theorem, we have

$$dE = TdS - PdV_s + \mu dN + \bar{\mu} d\bar{N} \quad (23)$$

where  $S$  is the entropy of the system,  $P$  is the external pressure,  $V_s$  is the total volume of the system,  $-d\bar{N}$  is the number of atoms attached onto the charged mesa, and  $dN$  is the number of atoms detached from the surrounding neutral mesas. We assume that in the mass flow process between the charged mesa and the neutral mesas, (1)  $dN = -d\bar{N}$ , (2) no volume work is done ( $PdV_s = 0$ ), and (3) the process is adiabatic ( $dS = 0$ ). Then, Eq. (23) can be written as

$$dE = \mu dN + \bar{\mu} d\bar{N} = (\mu - \bar{\mu}) dN \quad (24)$$

or

$$\mu - \bar{\mu} = \frac{dE}{dN} = \Omega \frac{dE}{dV} \quad (25)$$

If  $R$  is constant,  $dE/dV = (\partial E/\partial V)_R$ , and then comparing Eq. (25) with Eq. (14) yields

$$\mu - \bar{\mu} = \mu_H \quad (26)$$

Substituting Eq. (26) into Eq. (20), we have

$$\frac{dH}{dt} = -\frac{\sigma}{\pi R^2} \mu_H \quad (27)$$

Next, substituting Eq. (17) into Eq. (27) we get

$$\frac{dH}{dt} = \beta \frac{Q^2}{H^2} \quad (28)$$

where

$$\beta = \sigma \Omega \frac{\ln(R_g/R)}{4\pi^3 \varepsilon R^4} \quad (29)$$

Similar to the hemisphere model in Section 2.1, it can be proved that if the charge  $Q$  carried by the charged cylindrical mesa remains unchanged, the surrounding neutral mesas will completely disappear. However, if the substrate is a semiconductor, there will be a charging-discharging process, and consequently  $Q$  is time-dependent. Generally, the metal-semiconductor interface can be considered as a depletion-layer capacitor. If the depletion-layer capacitance is

assumed to be  $C_d$ , then when a charging voltage of  $U$  is applied, the maximum charge amount of the capacitor is

$$Q_0 = C_d U \quad (30)$$

The time-dependent charge carried by the metal mesa can be expressed as

$$Q(t) = \begin{cases} Q_0(1 - e^{-t/\tau_1}), & \text{for } 0 \leq t \leq t_1 \\ Q_1 e^{-(t-t_1)/\tau_2}, & \text{for } t \geq t_1 \end{cases} \quad (31)$$

where  $t_1$  is the total time of the charging process after which the applied voltage is removed and then the mesa discharges,  $\tau_1$  and  $\tau_2$  are, respectively, the time constants corresponding to the charging and discharging processes, and

$$Q_1 = Q_0(1 - e^{-t_1/\tau_1}) \quad (32)$$

which is the charge amount at  $t = t_1$  when the charging process terminates. The typical charging and discharging curve of a capacitor is shown in Fig. 3. The solid curve and the dashed curve, respectively, represent the charging and the discharging processes described in Eq. (31).

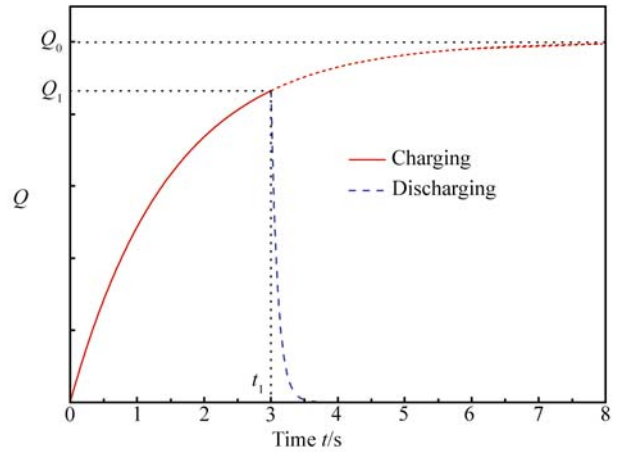


**Fig. 3** (Color online) Typical charging and discharging curve of a capacitor. The time constants are taken as  $\tau_1 = 1.5$  s and  $\tau_2 = 0.1$  s. The charging ending time is taken to be  $t_1 = 3$  s. The solid curve indicates the charging process, and the dashed curve indicates the discharging process. As  $\tau_1$  is chosen to be larger,  $Q_1$  will approach to  $Q_0$  along the short-dashed curve.

Substituting Eq. (31) into Eq. (28) results in the integration

$$\int_{H_0}^H H^2 dH = \beta \int_0^{t_1} Q_0^2 (1 - e^{-t/\tau_1})^2 dt + \beta \int_{t_1}^t Q_1^2 e^{-2(t-t_1)/\tau_2} dt \quad (33)$$

where  $H_0$  is the initial height of the charged mesa. From Eqs. (33) and (32), we obtain

$$H = \left\{ H_0^3 + 3\beta Q_0^2 \left[ t_1 - \frac{3}{2} \tau_1 - \frac{\tau_1}{2} e^{-2t_1/\tau_1} + 2\tau_1 e^{-t_1/\tau_1} + \frac{\tau_2}{2} (1 - e^{-t_1/\tau_1})^2 (1 - e^{-2(t-t_1)/\tau_2}) \right] \right\}^{1/3} \quad (34)$$

When  $t \rightarrow \infty$ , Eq. (34) becomes

$$H = \left\{ H_0^3 + 3\beta Q_0^2 \left[ t_1 - \frac{3}{2}\tau_1 - \frac{\tau_1}{2} e^{-2t_1/\tau_1} + 2\tau_1 e^{-t_1/\tau_1} + \frac{\tau_2}{2} (1 - e^{-t_1/\tau_1})^2 \right] \right\}^{1/3} \quad (35)$$

Here, we have assumed that there are a sufficient number of the neutral mesas surrounding the charged mesa for its height growth.

### 3 Explanations for experiments

#### 3.1 Selective growth of Pb nanomesas triggered by STM tip

Figure 4 shows the quick growth of a charged Pb mesa on Si(111). The experiment was by the Beijing Group [12] performed on an OMICRON UHV molecular beam epitaxy-STM system. About 3 monolayers of Pb were deposited on the clean Si(111)-(7 × 7) surface at ~ 150 K, forming flat-top mesas. The charging was applied at room temperature by a pulse of 10 V and a tunneling current 20 pA with feedback on for about several ms. Right after the pulse, normal room temperature STM scanning (1.5 V and 20 pA) was resumed to monitor the morphology evolution.

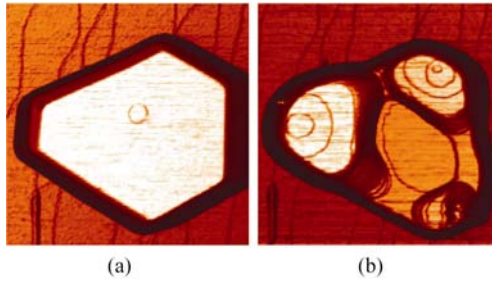


**Fig. 4** (Color online) The quick growth of a charged Pb mesa on Si(111). The charging STM tip is placed on the right foot of the mesa. The STM image size is 800 nm × 800 nm. **(a)** Before charging ( $t = 0$ ). **(b)** After charging ( $t \sim 30$  ms).

For an actual charged mesa, some mesa-edge positions have relatively higher charge distributions (the fringing effect) because these edge positions have relatively larger geometric curvatures. This indicates that the height growth first starts along these mesa-edge positions, creating many steps, as shown in Fig. 4. The charged mesa continues to grow even after discharging, since coarsening can now proceed via step flow without the need of nucleating new layers. The growth after discharging is much slower, as it is driven by a smaller chemical-potential difference due to mesa size

difference and by the tendency for the growing mesa to eliminate steps to resume the flat-top equilibrium shape. The growth stops when a flat top is formed. Further growth can be triggered only by another charging pulse. Below is a rough estimation for the increased height of the charged Pb mesa during the charging-discharging process. The time constants are defined by

$$\tau_1 = R_1 C_d \quad (36)$$

and

$$\tau_2 = R_2 C_d \quad (37)$$

where  $R_2$  is the interface resistance, and  $R_1$  is the sum of  $R_2$  and the STM contact resistance  $R_c$ . In experiments,  $R_2 \sim 10^3 \Omega$ ,  $R_c \sim 10^8 \Omega$ , and  $C_d \sim 10^{-16}$  F, so  $\tau_1 \sim 10^{-8}$  s, and  $\tau_2 \sim 10^{-13}$  s. Substituting these values of time constants into Eq. (31), the charging and discharging curves, respectively, can be plotted as Figs. (5) (a) and (b). The experimental charging ending time  $t_1 \sim 10^{-3}$  is much larger than  $\tau_1$  and  $\tau_2$ , so  $Q_1$  is close to  $Q_0$ , and Eq. (35) can be simplified as

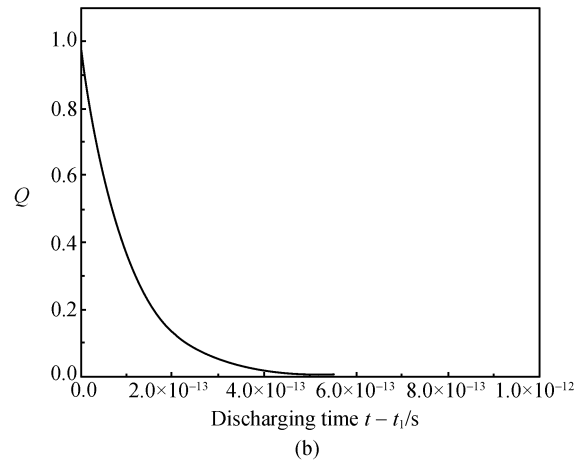
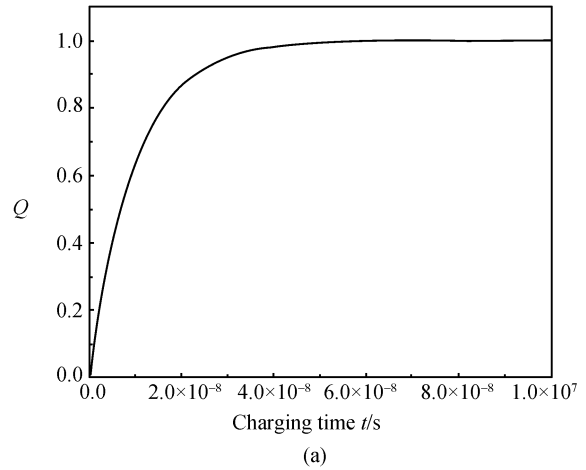


**Fig. 5** Charging and discharging curves of a Pb mesa on Si(111). The time constants:  $\tau_1 = 10^{-8}$  s, and  $\tau_2 = 10^{-13}$  s. The charging ending time  $t_1 = 10^{-3}$  s.  $Q$  is in unit of  $Q_0$ .

$$H = (H_0^3 + 3\beta Q_0^2 t_1)^{\frac{1}{3}} \quad (38)$$

This indicates that the main contribution to height growth is from the charging-saturation period ( $Q \approx Q_0$ ) in the charging process, and there are almost no contributions from the period *before* the charging-saturation as well as the *discharging* process. Typically, for the Pb and Si system in the experiment,  $\Omega \sim 0.03 \text{ nm}^3$ ,  $\Delta \sim 130 \text{ meV}$ , and  $\varepsilon \sim 2\varepsilon_0$ , where  $\varepsilon_0$  is the permittivity of free space, and according to Fig. 4, we take  $R \sim 300 \text{ nm}$ ,  $R_g/R \sim 10^3$ ,  $H_0 \sim 10 \text{ nm}$ ,  $U = 10 \text{ V}$ , and  $T = 300 \text{ K}$ . Substituting these parameters into Eq. (38) with the use of Eqs. (29), (22) and (30), we obtain a value of  $\Delta H = H - H_0 \sim 13 \text{ nm}$ , which agrees with the experimental measurement [12].

### 3.2 Fabrication of artificial nanowells with tunable size and shape by using STM

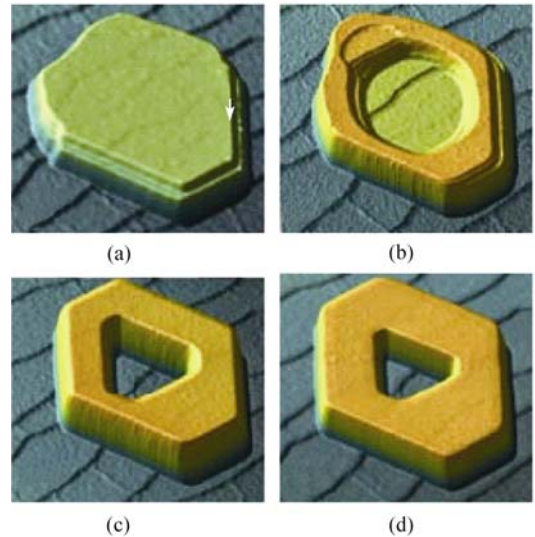
The construction of artificial nanostructures is of great significance in both the understanding of physical and chemical properties at nanoscale and potential nanodevice technologies. One effective way to construct artificial nanostructures is by using STM. In the early 1990s, STM was applied to move and position single atoms or molecules [13–17]. Larger nanostructures involving a huge quantity of atoms can be fabricated by self-organization growth [18–21], but the precise control in local structures is lacking in these studies. Recently, the STM manipulation based on the Coulomb sink effect has been applied to precisely control the thickness of the nanostructure with single atomic layer precision, and the engineered nanostructure can involve a macroscopic number of atoms up to  $10^5$ – $10^6$  [8, 12].

In this section, we illustrate a couple of examples of employing the Coulomb sink effect to extend the STM-based nanofabrication of metal structures. The experiments have been performed by the Beijing Group [22]. In the experiments, by applying a series of appropriate voltage pulses to the STM tip, the control of the lateral shape as well as the exact location of the targeted Pb island grown on Si(111)–(7 × 7) substrate can be achieved through regulating the pulse parameters. The resulting nanostructures have interesting shapes and selected locations with atomic layer precision, implying the potential in the research and application of size- and shape-sensitive properties at nanoscale.

In experiments, the high purity Pb is thermally evaporated from a homemade tungsten cell and deposited onto the Si(111)–(7 × 7) substrate, and the Pb mesas can be grown in an ultrahigh vacuum molecular beam epitaxy chamber. More details for the description of the instrument and experimental conditions have been reported [22, 23]. Here, we only

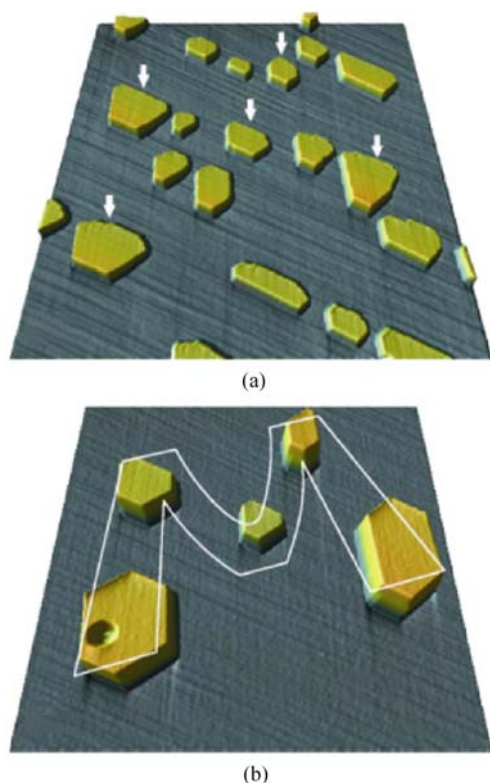
quote the most interesting experimental results to analyze how the Coulomb sink effect is functioning in the fabrication of nanostructures.

Figure 6 (a) shows a flat-top Pb mesa grown by depositing Pb at 150 K followed by slowly warming up to room temperature. The mesa height has a range of 3.1 nm to 4.9 nm from the upper left to the lower right due to the stepped Si(111) substrate surface. When a voltage pulse of  $\sim 10 \text{ V}$  is applied upon the mesa edge by the STM tip, as indicated by a white arrow in Fig. 6 (a), for 10 ms during scanning, the flat mesa top was triggered to grow around the edge at the same time, as shown in Fig. 6 (b). From the viewpoint of Coulomb sink effect, this is because when the charge is injected into the Pb mesa, the chemical potential of the mesa, especially around the mesa edge with a much larger curvature and therefore the much higher charge distribution, is drastically dropped, and then the mesa top edge is triggered to quickly grow at the expense of the neighboring neutral mesas. The outside profile of the nanowell remains nearly unchanged relative to the original mesa shown by Fig. 6 (a), and the nanowell bottom has the same height as that of the original flat-top mesa, but the height of the sidewall increases by 3.58 nm, which is approximately equal to 12 Pb(111) monolayers. This indicates that a center-half-hollowed nanowell is fabricated successfully with atomic layer precision. It is found by STM observation that such the center-half-hollowed nanostructure is very stable, even taking a couple of days to resume the flat top of the mesa if no further STM voltage pulse is applied on it.



**Fig. 6** (Color online) STM images ( $720 \text{ nm} \times 720 \text{ nm}$ ) showing the nanowells fabricated by the Beijing Group [22]. (a) Original Pb island before STM manipulation. (b) Center-half-hollowed nanowell formed by charging at the Pb mesa edge. (c) and (d) Center-full-hollowed nanowells formed by charging at the bottom of the nanowell in (b). The nanowells in (c) and (d) have different ratios of inner-outer diameter and thickness.

It is also possible that the Pb mesa transforms into some interesting shapes if a series of STM voltage pulses is applied at different sites on the top of the Pb mesa. When the center-half-hollowed nanowell shown in Fig. 6 (b) is manipulated with another STM voltage pulse at the bottom, the growth will start from the inner edge side where the charge distribution is much higher than the bottom due to the large curvature. The bottom is relatively neutral with the higher chemical potential due to the nearly zero curvature, and then completely broken up, so that the bottom atoms climb up and attach to the inner sidewall edge to reduce the local chemical potential. Thus, the center-half-hollowed nanowell becomes a center-full-hollowed structure finally, as shown in Fig. 6 (c). Unlike the center-half-hollowed nanowell, the inner sidewall of the center-full-hollowed nanowell forms a triangle or hexagon hole. This indicates that except for the Coulomb sink, the diffusion effect will also concurrently occur, which is related to the mass transition of inner walls from a stepped structure in the center-half-hollowed well to a faceted structure in the center-full-hollowed well. The inner-outer diameter ratio can be increased by charging the nanowell from the inner edge side, which makes the inner



**Fig. 7** (Color online) STM images ( $5000\text{ nm} \times 5000\text{ nm}$ ) showing the nanoarchitecture fabricated by the Beijing Group [22]. **(a)** Initial Pb (111) island archipelago obtained by depositing Pb atoms on the Si (111) surface. The arrows indicate the selected Pb islands to be manipulated. **(b)** The letter “M” written by growing five preselected Pb islands and erasing all others in **(a)** using STM.

Pb atoms climb up. The thickness can be tuned by charging from the outer edge side which induces mass transport from the surrounding neutral islands to the charged one. Figure 6 (d) shows the same nanowell but with tuned inner-outer diameter ratio and thickness by a series of STM voltage pulses. More details for how the size and shape of a nanowell depend on STM pulse parameters such as the amplitude or the time constant have been also reported in Ref. [22].

The above STM manipulation can be extended to fabricate predesigned nanoarray patterns even in the microscale [22]. Figure 7 shows an example, where five selected islands, indicated by the five white arrows in Fig. 7 (a), are made to grow, while all the others are “erased”, forming the letter “M”, as indicated by the white line in Fig. 7 (a). The mass conservation has been also checked, and consequently it is confirmed that the supply of atoms for the growth of selected islands comes from their neighboring islands.

## 4 Summary

We have demonstrated a new concept of the Coulomb sink to elucidate the coarsening of metal mesas on a surface. Charging reduces the chemical potential of the charged mesa, making it act as a Coulomb sink to grow at the expense of its neighboring neutral mesas. Thus, it triggers an otherwise ceased coarsening process. For the cylindrical mesas, by introducing a growth index function, we show that the charged mesa grows preferentially; its height and the growth proceeds first rapidly by nucleation of new layers around the island edge creating many steps, and then continues slowly via step flow after discharging to resume a flat top. The theory has successfully explained most salient qualitative features observed in the coarsening of charged Pb mesas on Si(111).

The Coulomb sink, leading to cluster agglomeration, is effectively a reversed process of Coulomb explosion leading to cluster fragmentation. It provides a unique and effective method for manipulating the growth of metal nanoclusters on semiconductor or insulator surface with a size control up to millions of atoms. Various nanostructures by “massive” STM manipulation of millions of atoms via the Coulomb sink effect have been created. In this way, large-scale nanostructures can be fabricated with high precision. The nanostructures so obtained have controllable shapes and sizes. An island array to build predesigned architectures by growing, moving, and erasing entire islands can also be manipulated.

**Acknowledgements** This work was supported by the National Science Foundation (Grant No. DMR-0307000). The calculations were performed on an AMD Opteron cluster at the CHPC, University of Utah.

---

**References**

1. L. Rayleigh, *Philos. Mag.*, 1882, 14: 184
2. F. Liu, M. R. Press, S. N. Khanna, and P. Jena, *Phys. Rev. Lett.*, 1987, 59: 2562
3. H. Okamoto, D. Chen, and T. Yamada, *Phys. Rev. Lett.*, 2002, 89: 256101
4. E. Bauer, *Z. Kristallogr.*, 1958, 110: 372
5. F. Liu, *Phys. Rev. Lett.*, 2002, 89: 246105
6. J. D. McBride, B. V. Tassell, R. C. Jachmann, and T. P. Beebe, Jr., *J. Phys. Chem. B*, 2001, 105: 3972
7. K. Thürmer, J. E. Reutt-Robey, and E. D. Williams, *Surf. Sci.*, 2003, 537: 123
8. C. -S. Jiang, et al., *Phys. Rev. Lett.*, 2004, 92: 106104
9. Y. Han, M. Hupalo, M. C. Tringides, and F. Liu, *Surf. Sci.*, 2008, 602: 62
10. S. -C. Li, Y. Han, J. -F. Jia, Q. -K. Xue, and F. Liu, *Phys. Rev. B*, 2006, 74: 195428
11. F. Liu, A. H. Li, and M. G. Lagally, *Phys. Rev. Lett.*, 2001, 87: 126103
12. Y. Han, et al., *Phys. Rev. Lett.*, 2004, 93: 106102
13. D. M. Eigler and E. K. Schweizer, *Nature*, 1990, 344: 524
14. T. -C. Shen, et al., *Science*, 1995, 268: 1590
15. L. Bartels, G. Meyer, and K.-H. Rieder, *Phys. Rev. Lett.*, 1997, 79: 697
16. B. C. Stipe, et al., *Phys. Rev. Lett.*, 1997, 78: 4410
17. J. K. Gimzewski and C. Joachim, *Science*, 1999, 283: 1683
18. K. Kern, et al., *Phys. Rev. Lett.*, 1991, 67: 855
19. T. M. Parker, L. K. Wilson, N. G. Condon, and F. M. Leibsle, *Phys. Rev. B*, 1997, 56: 6458
20. R. Nötzel, et al., *Nature*, 1998, 392: 56
21. M. Seul and D. Andelman, *Science*, 1995, 267: 476
22. S. -C. Li, et al., *Appl. Phys. Lett.*, 2006, 89: 123111
23. S. -C. Li, et al., *Phys. Rev. Lett.*, 2004, 93: 116103